Near-wall statistics of a turbulent pipe flow at shear Reynolds numbers up to 40,000

Christian E. Willert[1]†, Julio Soria[2,3], Michel Stanislas[4], Joachim Klinner[1], Omid Amili[2], Michael Eisfelder[2], Christophe Cuvier[4], Gabriele Bellani[5], Tommaso Fiorini[5] and Alessandro Talamelli[5]

[1]DLR Institute of Propulsion Technology, 51170 Köln, Germany

[2]LTRAC, Department of Aerospace and Mechanical Engineering, Monash University, Clayton, Australia

[3]Department of Aeronautical Engineering, King Abdulaziz University, Jeddah, Saudi Arabia

[4]LML, Ecole Centrale de Lille, France

[5]CIRI Aeronautics, University of Bologna, Italy

(Received xx; revised xx; accepted xx)

This paper reports on near wall two-component - two-dimensional (2C-2D) PIV measurements of a turbulent pipe flow at shear Reynolds numbers up to $Re_\tau = 40\,000$ acquired in the CICLoPE facility of the University of Bologna. The 111.5 m long pipe of 900 mm diameter offers a well-established turbulent flow with viscous length scales ranging from 85 μm at $Re_\tau = 5\,000$ down to 11 μm at $Re_\tau = 40\,000$. These length scales can be resolved with a high-speed PIV camera at image magnification near unity. Statistically converged velocity profiles were determined using multiple sequences of up to 70 000 PIV recordings acquired at sampling rates of 100 Hz up to 10 kHz. Analysis of the velocity statistics shows a well resolved inner peak of the streamwise velocity fluctuations that grows with increasing Reynolds number and an outer peak that develops and moves away from the inner peak with increasing Reynolds number.

1. Introduction

The flow of fluids around and inside solid bodies is ubiquitous in industry and transport with near wall turbulence being recognized as one of the key fundamental issue for the modelling of most of these flows of practical interest and representing the Achille's heel of turbulence models. This is partly due to the lack of reliable measurements very close to the wall at sufficiently high Reynolds numbers to be relevant for practical applications (Smits *et al.* 2011). Even the smallest hot wire probes have difficulties very close to the wall at high Reynolds number (Hultmark *et al.* 2013). An improved characterization and understanding of the very near wall turbulence is essential to build more reliable models and eventually provide the necessary knowledge to yield viable methods that will reduce drag, one of the key issues in the present context of energy savings.

The key problem in currently available measurements is that even in large facilities, the high Reynolds number leads to very small scales near the wall, which are impossible to resolve with the standard laboratory measurement tools that are currently employed around the world.

Previous experimental measurements of high-Re pipe flows are mainly available from Princeton's Super-Pipe facility Hultmark *et al.* (2012, 2013). Due to the small viscous length scales in this facility ($l^* = \nu/u_\tau < 1\,\mu$m at $Re_\tau = 70\,000$), measurements were

† Email address for correspondence: chris.willert@dlr.de

performed with specialized micro-fabricated hotwire probes (NSTAP). Yet even these probes have not been able to adequately resolve the velocity profile in the viscous layer immediately adjacent to the wall ($y^+ < 15$) as they had a length in viscous units, $l^+ = 60$, which is well beyond the maximum $l^+ = 20$ recommended by Ligrani & Bradshaw (1987) and Hutchins *et al.* (2009) to keep the error to less than 10% in the streamwise Reynolds stress. Information on the evolution of the inner turbulence peak, considered to be the primary source of turbulence production (Pullin *et al.* 2013), thus is very limited and inconclusive.

This type of information is available from DNS of turbulence pipe flow which have been performed by Ahn *et al.* (2015) for $Re_\tau \approx 3\,000$ and for channel flow up to $Re_\tau \approx 5\,200$ by Lee & Moser (2015). The Reynolds number of these simulations still are an order of magnitude smaller than the currently available high-Re_τ pipe flow experiments. At these lower Reynolds numbers the so-called outer peak starts to appear but does not yet exhibit a distinct peak or plateau (it appears around $Re_\tau \approx 20\,000$).

Aside from the data available from the Princeton SuperPipe, wall-normal profiles of the streamwise Reynolds stress have been measured by Schultz & Flack (2013) for channel flows up to $Re_\tau = 6\,000$, indicating that the inner peak increases with increasing Reynolds number. A trend that thus far could not be confirmed for pipe flows at similar or higher Reynolds numbers. However, it is also worth noting that in the Schultz & Flack (2013) study, which used laser Doppler velocimetry (LDV), the viscous length scale of $l^* = 2\,\mu$m at $Re_\tau = 6\,000$ only allowed for measurements down to $y^+ \approx 20$.

In this paper we report on two-component - two-dimensional (2C-2D) near wall velocity measurements of turbulent pipe flow at shear Reynolds numbers ranging between $Re_\tau = 5\,000 - 40\,000$ acquired in the Long Pipe facility in CICLOPE (Center for International Cooperation in Long Pipe Experiments) of the University of Bologna, located in Predappio, Italy (Talamelli *et al.* 2009; Örlü *et al.* 2017). As a consequence of the installation site and the characteristic dimensions of the facility, the Long Pipe offers viscous length scales that can be resolved using conventional imaging hardware. Despite the fact that spatial resolution effects prevent accurate measurements of the streamwise variance at the inner peak for Reynolds number above 28 000, the resolution is sufficient to determine the increasing trend of the inner peak. However, more generally, the new 2C-2D near wall measurements reported here, represent the highest spatial resolution (u, v) velocity measurements up to $Re_\tau = 40\,000$ compared to previous published results (Hutchins *et al.* 2009; Hultmark *et al.* 2013; Örlü *et al.* 2017) - noting that Hutchins *et al.* (2009); Hultmark *et al.* (2013) only measured the streamwise u-velocity component, while Örlü *et al.* (2017) measured the (u, v)-velocity components at selected points using their probe.

2. Experimental technique

2.1. *CICLoPE facility*

The Long Pipe (LP) is a unique facility to study high Reynolds number, fully developed turbulent pipe flow. With a diameter of 0.9 m and a length of 111.5 m, the LP operates with air at ambient pressure in closed loop with a 200kW axial fan in the return duct (Figure 1). A cooling unit ensures temperature stability within $\pm 0.1^o$C. The LP is made of 5 m long carbon-fibre sections with a surface roughness $k_{\rm rms} \approx 0.2\mu$m. At centreline velocities between 5 and 40 m/s the turbulent pipe flow has viscous length scales ranging from $l^* = 85\mu$m at $Re_\tau = 5\,000$ down to $l^* = 11\mu$m at $Re_\tau = 40\,000$. The wall friction τ_w is determined by a linearly fitting 6 static pressure measurements in the last portion

FIGURE 1. Photograph of the 111.5 m long CICLoPE facility with the measurement location seen at the far end.

of the LP ($88 < L/D < 122$), where the flow is assumed to be fully-developed. The static pressure is measured through 1 mm wall taps placed with a 5 m spacing along the pipe. The estimated uncertainty in τ_w is below $\pm 0.25\%$ as reported in Fiorini (2017).

2.2. *PIV technique*

The reported length scales of $l^* = 11 - 85\,\mu$m can be resolved with a high-speed PIV camera at image magnification near unity. The employed PIV measurement approach closely follows the procedures and methods laid out by Willert (2015) to capture the the wall-normal velocity profile and higher order statistics. The near-wall measurement approach has been successfully used in a variety of previous applications however with viewing arrangements involving straight walls (Soria *et al.* 2016; Cuvier *et al.* 2017). To apply the technique in the curved convex contour of the pipe required the design of a new imaging approach. In order to obtain a reasonably orthogonal view of the near wall region a specific circular insert was designed to accommodate a thin 45^o high-aspect mirror that was placed about 50 mm from the area of interest (Figure 2, right). While the mirror does protrude into the flow it has a low cross-section (1 mm thickness), considered to have only a minor influence in the imaged domain.

The imaging setup was designed for a magnification of unity (m = 1.0) using a macroscopic lens of 200 mm focal length (Nikon Micro-Nikkor 200/4) at a maximum aperture of $f^{\#} = 5.6$. During the measurements the aperture could be reduced to $f^{\#}$ ranging from 8 - 11 due to the high energy levels provided by a pulsed, high speed laser (Quantronix Darwin Duo), resulting in an estimated depth of field ranging from 660 μm at $f^{\#} = 8$ to 1.26 mm at $f^{\#} = 11$. The approximately $300 \pm 100\,\mu$m thin laser light sheet was introduced radially into the pipe (Figure 2, left). Thus, the size of the measurement volume in the direction normal to the streamwise-wall-normal plane is given by the thickness of the laser sheet. The PIV image acquisition was undertaken using a high-speed camera with a 4 megapixel CMOS sensor (PCO AG, DIMAX-S4), which has a pixel pitch of 11 μm. Using macroscopic imaging at unity the smallest viscous scales at the facility design point of $Re_\tau = 40\,000$ match the pixel size. The field of view of the camera was reduced to 178 or 200 pixel width and varied in height between 1008 and 2016 pixels. This reduction allowed an increase of the number of acquired image pairs (*i.e.* velocity fields) to more than 70 000 during a single run.

Seeding of 1 μm droplets was provided globally for the PIV experiments via a smoke

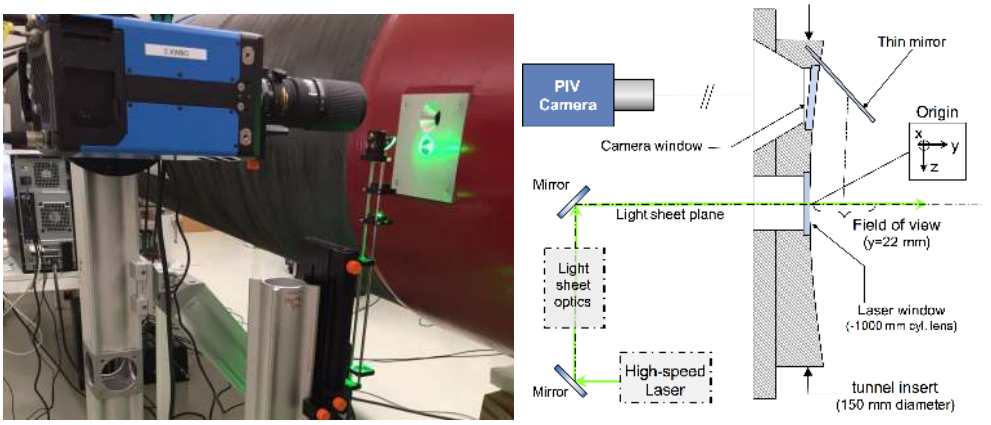

FIGURE 2. Photograph of the PIV setup on the CICLoPE facility (left), schematic of insert for near-wall PIV measurements (right) with coordinate system used for the investigation.

generator using a water-glycol mixture, which was injected into the flow downstream of the test section, allowing it to mix thoroughly before reaching the measurement area after running the full length of the return duct and pipe.

2.3. *Acquired data*

PIV measurement were performed at five Reynolds number as summarised in Table 1, which also shows the details of the measurement volume for the PIV in viscous units, which, as already pointed out, is controlled by the laser sheet thickness, which is always smaller that the depth-of-field.

Statistically converged velocity profiles could be achieved using up to 70 000 samples per sequence acquired at low laser repetition rates (100 Hz). Higher sampling rates of 10 kHz provide temporally coherent data from which frequency spectra can be obtained.

With increasing Reynolds number (U_c = 30 - 40 m/s) a slight vibration was observed in the image data through a fluctuation of the wall position of up to 5 pixels peak-to-peak ($\approx 50\,\mu$m) (Figure 3, left). The vibration had a constant fundamental frequency of about 670 Hz throughout the duration of the measurement campaign and was found to be independent of the Reynolds number (Figure 3, right). It is not possible, without further studies, to determine if this small vibration is due to a vibration of the pipe structure or of the optical set-up, as both would result in the observed relative wall motion. Nonetheless, this offset must be accounted for prior to analysis to warrant reliable data in the immediate vicinity of the wall. Using an image correlation approach the motion of the wall was tracked to better than ± 0.1 pixel, *i.e.* better than $\pm 0.1^+$ at the highest Reynolds number. This displacement data was used to offset the images prior to PIV processing.

The image data was processed using a multigrid/multipass 2C-2D cross-correlation PIV analysis algorithm (Willert & Gharib 1991; Soria 1996) with measurement volumes of 6 pixel in wall-normal direction corresponding to 0.8^+ at $Re_\tau = 5\,400$ and increasing to 6.1^+ at $Re_\tau = 40\,000$. In the streamwise direction the measurement volume has a length of 64 pixels (700 μm), introducing minor spatial filtering, while in the spanwise direction the measurement volume is controlled by the approximately 300μm thin laser sheet, which also introduces minor spatial filtering. Full details of these measurement parameters and other pertinent experimental parameters are provided in Table 1, which

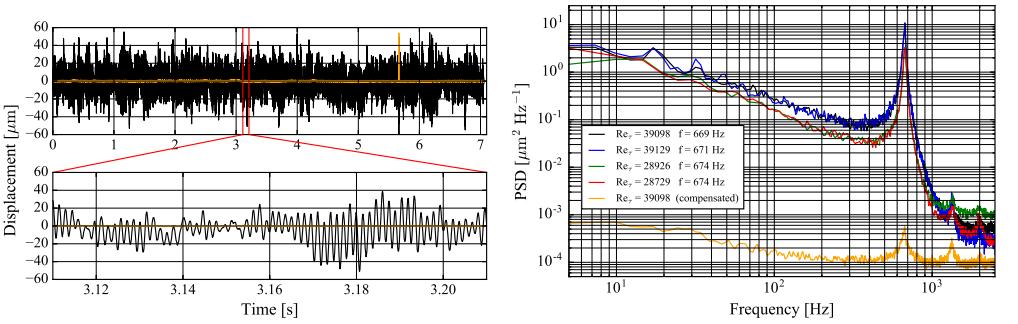

FIGURE 3. Time trace of the detected vibration at $Re_\tau \approx 40\,000$ (left) acquired at 10 kHz. Orange line indicates detected residual vibration after image offset procedure. Right: vibration spectra for different image sequences.

Bulk velocity	U_c	**4.6**	**10.9**	**19.5**	**28.1**	**40.5**	**m/s**
Reynolds number	Re_τ	5 400	11 600	20 000	28 000	40 000	
Pressure gradient	dP/dx	0.174	0.810	2.34	4.62	9.17	Pa/m
Friction velocity	u_τ	0.180	0.395	0.672	0.943	1.332	m/s
Viscous scale	ν/u_τ	85	39	22	16	11	μm
Effective PIV measurement	IW_{x^+}	8.72	19.0	32.2	45.3	64.7	$^+$
volume size	IW_{y^+}	0.82	1.78	3.02	4.25	6.06	$^+$
	IW_{z^+}	3.5	7.7	13.6	18.8	27.3	$^+$
Number of sequences		1	3	3	3	3	
Samples/Sequence ($f_{\mathrm{acq}} = 100$ Hz)	N	35 265	35 265	35 265	35 265	35 265	
Samples/Sequence ($f_{\mathrm{acq}} = 10$ kHz)	N	35 265	70 512	70 512	70 512	70 512	
Independent samples at 100 Hz	N_{eff}	9 670	49 600	83 600	97 695	97 695	
Uncertainty in $\overline{U}$ ($y > 1$ mm)	$\epsilon_{\overline{U}}$	0.32%	0.13%	0.09%	0.08%	0.08%	
Uncertainty in $\sqrt{\langle u'u' \rangle}$ ($y > 1$ mm)	$\epsilon_{u'}$	1.4%	0.65%	0.50%	0.45%	0.45%	
Filtering of $\langle u'u' \rangle$ at $y^+ = 15$		-0.25%	-1%	-2.5%	-4.5%	-7.5%	
Noise estimate at $y^+ = 15$	$\epsilon_{n_{u'u'}}$	1%	1%	1%	2%	2%	
Filtering of $\langle u'u' \rangle$ at $y^+ = 200$		-0.2%	-0.4%	-1%	-2%	-3%	
Noise estimate at $y^+ = 200$	$\epsilon_{n_{u'u'}}$	1.6%	1.4%	1.3%	2.4%	2.2%	

TABLE 1. PIV acquisition parameters for near-wall turbulent pipe flow measurements

as mentioned above represent the highest spatial resolution (u, v) near wall velocity measurements for $Re_\tau = 5\,400$ - $40\,000$.

To support this argument, the missing energy due to PIV filtering is coupled to the finite volume PIV interrogation that was estimated with the 1D transfer function of PIV for the streamwise spectrum as proposed by Foucaut *et al.* (2004) applied to hot-wire spectrum of boundary layer obtained by Carlier & Stanislas (2005). The difference of the integral of the filtered spectrum compared to original one can be considered the best estimation of the missing energy and the result is given in Table 1 for $y^+ = 15$ and 200. Also provided is the PIV noise part which overestimates $\langle u'^2 \rangle^+$ for these two wall normal positions.

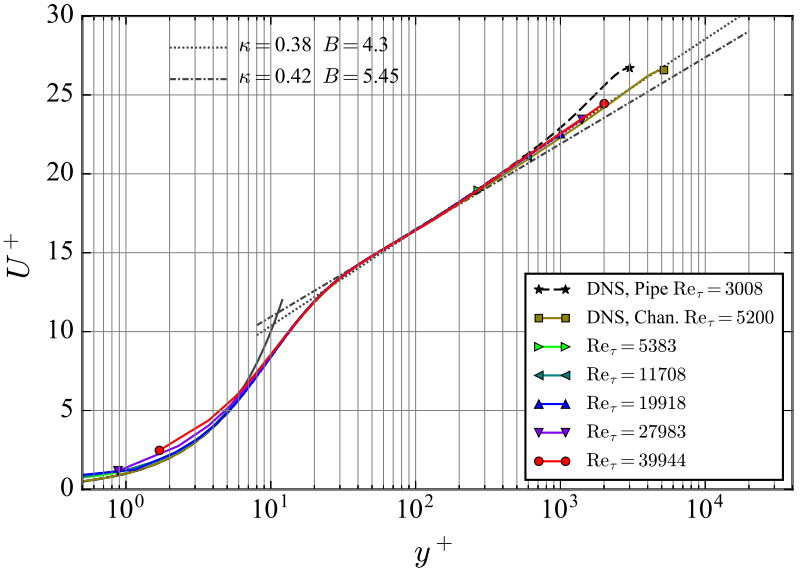

FIGURE 4. Mean streamwise velocity scaled with inner coordinates. DNS of turbulent pipe flow at $Re_\tau = 3008$ by Ahn *et al.* (2015), DNS of turbulent channel flow data at $Re_\tau = 5200$ by Lee & Moser (2015).

3. Results and Discussion

The profiles of the mean velocity and measured Reynolds stresses shown in Figures 4 and 5, respectively, show that they only differ marginally from those of turbulent channel flows and flat plate boundary layers from the wall up through the logarithmic layer. The mean streamwise velocity profiles are fairly consistent across all Reynolds numbers and in good agreement with the DNS channel flow results of Lee & Moser (2015). A clear log region is also observable. Figure 6 shows the indicator functions for a power law (left) and a log law (right). It does not show a consistently strict plateau region for either case. Although there is less scatter in the power law indicator function shown in Figure 6 (left), there is no horizontal plateau region for $y^+ > 200$ and whilst the log indicator function has more scatter, there is an approximate plateau region for $200 < y^+ < 2000$ observable, which is consistent with the DNS channel flow results of Lee & Moser (2015), who found an approximate plateau in the log indicator function between $y^+ = 350$ and $y^+ = 830$.

As far as the Reynolds stresses are concerned, the data show a well resolved inner peak of the streamwise velocity fluctuations $\langle u'^2 \rangle^+$ that grows with increasing Reynolds number (see insert of Figure 5), which so far was not clearly documented in previous measurements of high-Re pipe flows such as the Princeton SuperPipe (see e.g. Hultmark *et al.* (2012); Vallikivi *et al.* (2015)), most likely due to lack of spatial resolution. For comparison two profiles of the streamwise velocity fluctuations $\langle u'^2 \rangle^+$ acquired in the SuperPipe using NSTAP hotwire probes are presented in Figure 5, bottom.

The PIV data also provides the wall-normal velocity component v from which two additional terms of the Reynolds stress tensor can be computed. Shown in Figure 5, top, the plateaus of $\langle v'^2 \rangle^+$ and $\langle u'v' \rangle^+$ extend significantly with increasing Re_τ with the ends not captured due to the limited field of view.

At $Re_\tau = 5400$ both the profile and the maximum of $\langle u'^2 \rangle^+$ or *inner peak* matches

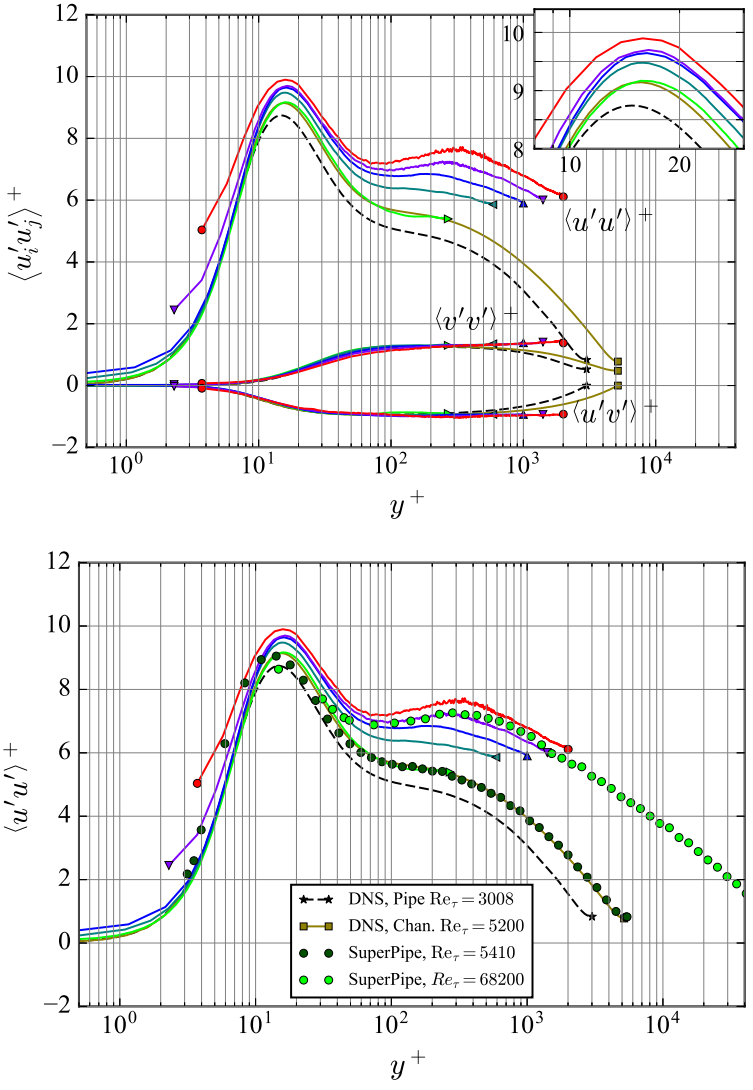

FIGURE 5. Variances and co-variances of the streamwise and wall-normal velocity components. DNS of turbulent pipe flow at $Re_\tau = 3008$ by Ahn *et al.* (2015), DNS of turbulent channel flow data at $Re_\tau = 5200$ by Lee & Moser (2015). Bottom: variance of streamwise velocity in comparison to NSTAP data obtained in the SuperPipe Hultmark *et al.* (2013); all other symbols as in Figure 4

the DNS channel flow data at $Re_\tau = 5\,200$ by Lee & Moser (2015). Figure 7 shows that with increasing Re_τ the maximum departs from extrapolations made from DNS channel flow data by Lozano-Durán & Jiménez (2014) and Lee & Moser (2015) and for turbulent boundary layers by Sillero *et al.* (2014). The present data suggests a nonlinear trend of the inner peak magnitude with Reynolds number which has to be taken with precaution as the filtering effects increase with Reynolds number (-5.5% at the maximum Re_τ studied).

As far as the peak position of $\langle u'^2 \rangle^+_{max}$ with respect to the wall is concerned, the DNS predicts an increase with Re_τ (insert in Figure 7), which can be clearly observed in the

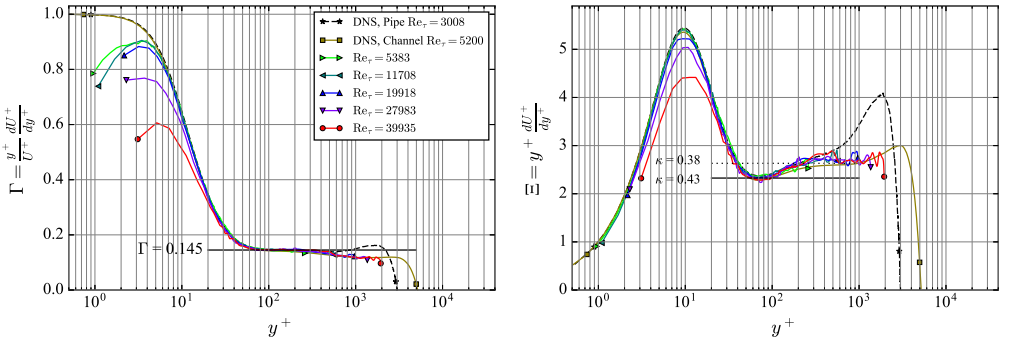

FIGURE 6. Wall-normal distributions of the power law (left) and log law indicator functions (right). DNS of turbulent pipe flow at $Re_\tau = 3008$ by Ahn *et al.* (2015), DNS of turbulent channel flow data at $Re_\tau = 5200$ by Lee & Moser (2015).

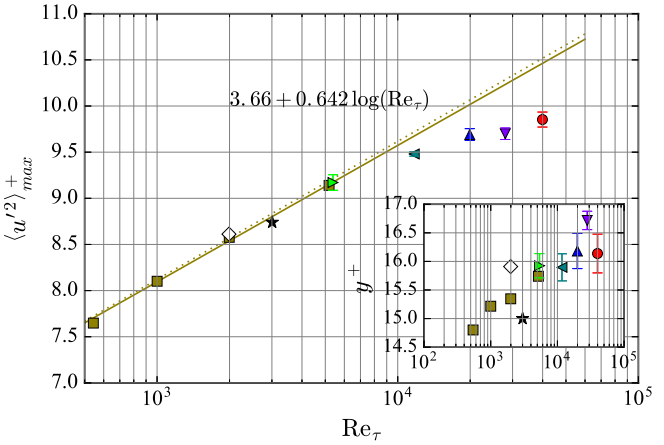

FIGURE 7. Dependence of the variance maximum of u on Reynolds number Re_τ and wall-normal location of maximum (insert). Square symbols (□) and predicted relationship (solid line) from DNS by Lee & Moser (2015), dotted line by Lozano-Durán & Jiménez (2014), (⋆) DNS of turbulent pipe flow at $Re_\tau = 3008$ by Ahn *et al.* (2015), (◇) DNS of turbulent boundary layer at $Re_\tau = 2000$ by Sillero *et al.* (2014).

present measurements. However, there is some scatter in the peak location due to the finite sampling spacing of 2.0 pixel in y corresponding to 2^+ at $Re_\tau = 40\,000$. Finer spatial sampling and/or peak fitting may improve the estimates of both the position and the magnitude of $\langle u'^2\rangle^+_{max}$.

As shown in Figure 5, although limited to the lower 20 mm of the pipe (*i.e.* $y/R \leqslant 0.044$), the spatial domain of the present measurements is sufficient to also document the steady growth of the outer peak of the streamwise Reynolds stresses. A distinct outer peak clearly develops with increasing Re_τ and is observable for $Re_\tau \geqslant 20\,000$. This outer peak is found to shift away from the inner peak with Re_τ, a behaviour that is in good agreement with data acquired in the SuperPipe facility (Hultmark *et al.* 2012; Vallikivi *et al.* 2015) (see also Figure 5, bottom).

Consideration of the wall-normal distribution of the integral time scales of U estimated through integration of the autocorrelation of the streamwise velocity (Pope 2000) indicates that only the measurements for $Re_\tau = 30\,000$ and $40\,000$ are uncorrelated when

acquired at $f_{\mathrm{acq}} = 100\,\mathrm{Hz}$. For all other sequences the number of effective samples N_{eff} is lower than N_{tot} and is used for the uncertainty estimates provided in Table 1. Following Benedict & Gould (1996) the uncertainty of both the mean and standard deviation of the streamwise velocity is based on a 95% confidence interval, which is estimated from N_{eff} and the estimated single sample uncertainty of the measured velocity σ_u at the 95% confidence level using:

$$\epsilon_{\overline{U}} = \frac{1.96}{\overline{U}}\sqrt{\frac{\sigma_u^2}{N_{\mathrm{eff}}}}, \qquad \epsilon_{u'} = \frac{1.96}{\sqrt{\langle u'u'\rangle}}\sqrt{\frac{\sigma_u^2}{2N_{\mathrm{eff}}}} \tag{3.1}$$

4. Concluding remarks

The combination of a facility offering relatively large viscous scales at high Reynolds number and a specifically adapted implementation of PIV enabled 2C-2D velocity measurements with high spatial and temporal resolution. This allowed for the first time a characterisation of the near wall velocity statistics of turbulent pipe flow at $Re_\tau upto 40\,000$, that are beyond the reach of current DNS and thus far could not be resolved in other facilities operating at similar Reynolds number, due to the much reduced viscous scales present there. These new data acquired in the CICLoPE facility not only show the emergence of the outer peak as observed in previous studies (*e.g.* Princeton's Superpipe), but also provides evidence of the persistence of the inner peak of the streamwise fluctuation, with a consistently higher amplitude than the outer peak. This inner peak is likely to continue to grow at even higher Reynolds numbers, possibly not to be overtaken by the outer peak. In the near wall region up into the logarithmic layer the distribution of the streamwise variance is very similar to that of a flat plate turbulent boundary layer. However, recent hot-wire measurements performed in the same facility show that after applying a correction for lack of spatial resolution, the outer peak resembles more a plateau than a peak (Fiorini 2017). Thus, although the present 2C-2D PIV measurements do not suffer to the same extent from spatial filtering, no firm conclusion about the existence and scaling of the outer peak can be made. However, it is found that the streamwise turbulent energy increases in this outer plateau or peak region with increasing Reynolds number.

As part of the EuHIT project the data presented in this article will be made available on the EuHIT TurBase Knowledge Base (https://www.euhit.org/infrastructures/turbase-knowledge-base).

Acknowledgements

The authors would like to acknowledge the financial support provided through the "European High performance Infrastructures in Turbulence" (EuHIT) Transnational Access Program (European Grant Agreement no. 312278). The visiting team would like to acknowledge the strong support and friendly atmosphere provided by the CICLoPE group during the entire test campaign (https://www.euhit.org/projects/HoloPipe).

REFERENCES

Ahn, J, Lee, J H, Lee, J, Kang, J-H & Sung, H J 2015 Direct numerical simulation of a 30R long turbulent pipe flow at $\mathrm{Re}_\tau = 3008$. *Physics of Fluids* **27** (6), 065110.

Benedict, L H & Gould, R D 1996 Towards better uncertainty estimates for turbulence statistics. *Experiments in Fluids* **22** (2), 129–136.

Carlier, J & Stanislas, M 2005 Experimental study of eddy structures in a turbulent boundary layer using particle image velocimetry. *Journal of Fluid Mechanics* **535**, 143188.

Cuvier, C., Srinath, S., Stanislas, M., Foucaut, J. M., Laval, J. P., Kähler, C. J., Hain, R., Scharnowski, S., Schröder, A., Geisler, R., Agocs, J., Röse, A., Willert, C., Klinner, J., Amili, O., Atkinson, C. & Soria, J. 2017 Extensive characterization of a high reynolds number decelerating boundary layer using advanced optical metrology. *Journal of Turbulence* **accepted**.

Fiorini, T. 2017 Turbulent pipe flow - high resolution measurements in CICLoPE. PhD thesis, University of Bologna.

Foucaut, J M, Carlier, J & Stanislas, M 2004 PIV optimization for the study of turbulent flow using spectral analysis. *Measurement Science and Technology* **15** (6), 1046.

Hultmark, M., Vallikivi, M., Bailey, S. C. C. & Smits, A. J. 2012 Turbulent pipe flow at extreme reynolds numbers. *Phys. Rev. Lett.* **108**, 094501.

Hultmark, M, Vallikivi, M, Bailey, S C C & Smits, A J 2013 Logarithmic scaling of turbulence in smooth- and rough-wall pipe flow. *Journal of Fluid Mechanics* **728**, 376–395.

Hutchins, N, Nickels, T B, Marusic, I & Chong, M S 2009 Hot-wire spatial resolution issues in wall-bounded turbulence. *Journal of Fluid Mechanics* **635**, 103–136.

Lee, M & Moser, R D 2015 Direct numerical simulation of turbulent channel flow up to $\mathrm{Re}_\tau \approx 5200$. *Journal of Fluid Mechanics* **774**, 395–415.

Ligrani, P M & Bradshaw, P 1987 Spatial resolution and measurement of turbulence in the viscous sublayer using subminiature hot-wire probes. *Experiments in Fluids* **5** (6), 407–417.

Lozano-Durán, A & Jiménez, J 2014 Effect of the computational domain on direct simulations of turbulent channels up to $\mathrm{Re}\tau = 4200$. *Physics of Fluids* **26** (1), 011702–7.

Örlü, R., Fiorini, T., Segalini, A., Bellani, G., Talamelli, A. & Alfredsson, P. H. 2017 Reynolds stress scaling in pipe flow turbulence—first results from CICLoPE. *Philosophical Transactions of the Royal Society of London A: Mathematical, Physical and Engineering Sciences* **375** (2089).

Pope, S B 2000 *Turbulent Flows*. Cambridge Univ. Press, Cambridge, UK.

Pullin, D I, Inoue, M & Saito, N 2013 On the asymptotic state of high reynolds number, smooth-wall turbulent flows. *Physics of Fluids* **25** (1), 015116–10.

Schultz, M P & Flack, K A 2013 Reynolds-number scaling of turbulent channel flow. *Physics of Fluids* **25** (2), 025104.

Sillero, J A, Jimenez, J & Moser, R D 2014 Two-point statistics for turbulent boundary layers and channels at reynolds numbers up to $\delta^+ \approx 2000$. *Physics of Fluids* **26** (10), –.

Smits, A J, McKeon, B J & Marusic, I 2011 High-Reynolds Number Wall Turbulence. *Annual Review of Fluid Mechanics* **43** (1), 353–375.

Soria, J 1996 An investigation of the near wake of a circular cylinder using a video-based digital cross-correlation particle image velocimetry technique. *Experimental Thermal and Fluid Science* **12**, 221–233.

Soria, J, Willert, C, Amili, O, Klinner, J, Atkinson, C, Stanislas, M, Schröder, A, Geisler, R, Agocs, J, Röse, A, Kähler, C J, Scharnowski, S, Hain, R, Foucaut, J M, Cuvier, C, Srinath, S & Laval, J P 2016 Spatially and temporally resolved 2C-2D PIV in the inner layer of a high reynolds number adverse pressure gradient turbulent boundary layer. In *18th International Symposium on the Application of Laser and Imaging Techniques to Fluid Mechanics, Lisbon (Portugal), July 4 -7, 2016*.

Talamelli, A, Persiani, F, Fransson, J H M, Alfredsson, P H, Johansson, A V, Nagib, H M, Redi, J-D, Sreenivasan, K R & Monkewitz, P A 2009 CICLoPE – a response to the need for high Reynolds number experiments. *Fluid Dynamics Research* **41** (2), 021407.

Vallikivi, M, Ganapathisubramani, B & Smits, A J 2015 Spectral scaling in boundary layers and pipes at very high reynolds numbers. *Journal of Fluid Mechanics* **771**, 303–326.

Willert, C E 2015 High-speed particle image velocimetry for the efficient measurement of turbulence statistics. *Experiments in Fluids* **56** (1).

Willert, C E & Gharib, M 1991 Digital particle image velocimetry. *Experiments in Fluids* **10**, 181–193.